



HAL
open science

Spin transitions in $\text{La}_{0.7}\text{Ba}_{0.3}\text{CoO}_3$ thin films revealed by combining Raman spectroscopy and X-ray diffraction

Zied Othmen, O. Copie, Kais Daoudi, Michel Boudard, Pascale Gemeiner, Meherzi Oueslati, Brahim Dkhil

► To cite this version:

Zied Othmen, O. Copie, Kais Daoudi, Michel Boudard, Pascale Gemeiner, et al.. Spin transitions in $\text{La}_{0.7}\text{Ba}_{0.3}\text{CoO}_3$ thin films revealed by combining Raman spectroscopy and X-ray diffraction. *Journal of Applied Physics*, 2016, 120, pp.015308. 10.1063/1.4955220 . hal-01385340

HAL Id: hal-01385340

<https://hal.science/hal-01385340>

Submitted on 27 Aug 2020

HAL is a multi-disciplinary open access archive for the deposit and dissemination of scientific research documents, whether they are published or not. The documents may come from teaching and research institutions in France or abroad, or from public or private research centers.

L'archive ouverte pluridisciplinaire **HAL**, est destinée au dépôt et à la diffusion de documents scientifiques de niveau recherche, publiés ou non, émanant des établissements d'enseignement et de recherche français ou étrangers, des laboratoires publics ou privés.

Spin transitions in $\text{La}_{0.7}\text{Ba}_{0.3}\text{CoO}_3$ thin films revealed by combining Raman spectroscopy and X-ray diffraction

Cite as: J. Appl. Phys. **120**, 015308 (2016); <https://doi.org/10.1063/1.4955220>

Submitted: 08 November 2015 . Accepted: 06 June 2016 . Published Online: 07 July 2016

Zied Othmen, Olivier Copie, Kais Daoudi, Michel Boudard, Pascale Gemeiner, Meherzi Oueslati, and Brahim Dkhil



View Online



Export Citation



CrossMark

ARTICLES YOU MAY BE INTERESTED IN

[Transport mechanism through metal-cobaltite interfaces](#)

Applied Physics Letters **109**, 011603 (2016); <https://doi.org/10.1063/1.4955204>

[Ferromagnetism in tetragonally distorted \$\text{LaCoO}_3\$ thin films](#)

Journal of Applied Physics **105**, 07E503 (2009); <https://doi.org/10.1063/1.3059606>

[Ferromagnetic spin-correlations in strained \$\text{LaCoO}_3\$ thin films](#)

Applied Physics Letters **93**, 212501 (2008); <https://doi.org/10.1063/1.3027063>

Lock-in Amplifiers
up to 600 MHz



Watch



Spin transitions in $\text{La}_{0.7}\text{Ba}_{0.3}\text{CoO}_3$ thin films revealed by combining Raman spectroscopy and X-ray diffraction

Zied Othmen,¹ Olivier Copie,² Kais Daoudi,^{1,3} Michel Boudard,⁴ Pascale Gemeiner,² Meherzi Oueslati,¹ and Brahim Dkhil²

¹Unité Nanomatériaux et Photonique, Faculty of Sciences of Tunis, Tunis El-Manar University, 2092 Tunis, Tunisia

²Laboratoire Structures, Propriétés et Modélisation des Solides, Centrale Supélec, CNRS-UMR 8580, Université Paris-Saclay, France

³Department of Applied Physics and Astronomy, College of Sciences, University of Sharjah, P.O. Box 27272, Sharjah, United Arab Emirates

⁴Univ. Grenoble Alpes, LMGP, F-38000 Grenoble, France

(Received 8 November 2015; accepted 6 June 2016; published online 7 July 2016)

In cobaltite, the spin states transitions of $\text{Co}^{3+/4+}$ ions govern the magnetic and electronic conduction properties. These transitions are strain-sensitive and can be varied using external parameters, including temperature, hydrostatic pressure, or chemical stresses through ionic substitutions. In this work, using temperature dependent Raman spectroscopy and X-ray diffraction, the epitaxial strain effects on both structural and vibrational properties of $\text{La}_{0.7}\text{Ba}_{0.3}\text{CoO}_3$ (LBCO) cobaltite thin films are investigated. All Raman active phonon modes as well as the structure are found to be strongly affected. Both Raman modes and lattice parameter evolutions show temperature changes correlated with magnetic and electronic transitions properties. Combining Raman spectroscopy and X-ray diffraction appears as a powerful approach to probe the spin transition in thin film cobaltite. Our results provide insight into strong spin-charge-phonon coupling in LBCO thin film. This coupling manifests as vibrational transition with temperature in the Raman spectra near the ferromagnetic spin ordered transition at 220 K. *Published by AIP Publishing.* [<http://dx.doi.org/10.1063/1.4955220>]

I. INTRODUCTION

The physics of hole-doped perovskite cobaltites $\text{La}_{1-x}\text{M}_x\text{CoO}_3$ ($\text{M} = \text{Ca}, \text{Sr}, \text{Ba}$) illustrates the richness and plethora of properties in transition metal oxides. It stimulates a lot of interest owing to their magnetic and electronic transport properties, making them potential candidates for future devices in the field of oxide electronics, like thermoelectric power generation,¹ solid oxide fuel cells,² and spintronic.³ The perovskite cobaltites exhibit fascinating properties that include competing magnetic ground states and their relationship with the Co spin state transition owing interesting electronic transport properties.⁴ The spin state transition in the LaCoO_3 was actively studied. In fact, the question whether intermediate spin (IS) indeed realized in this system keeps attention and remains a controversial topic for the last 50 years.^{5–7} LaCoO_3 exhibits two broad transitions: there is first a spin-state crossover at spin-state transition (between ~ 50 and 100 K), where a hump in the magnetic susceptibility signals the appearance of a paramagnetic semiconductor. The second one is an insulator-metal transition (TIM) between ~ 500 and 600 K.^{8,9} The parent LaCoO_3 compound is characterized by various Co ion spin states because of the competition between the crystal-field splitting energy Δ_{cf} and the intra-atomic (Hund) exchange interaction J_{ex} . As a consequence, three spin states associated with Co^{3+} ($3d^6$) t_{2g} and e_g orbital occupancy are permitted: low spin (LS), i.e., $t_{2g}^6e_g^0$ ($S=0$), IS, i.e., $t_{2g}^5e_g^1$ ($S=1$), and high spin (HS) state, i.e., $t_{2g}^4e_g^2$ ($S=2$).¹⁰ As a matter of fact, LaCoO_3 for instance displays different transitions between these spin states as a

function of temperature, which are characterized by a change of both magnetic susceptibility and conducting behavior. At low temperature, LaCoO_3 is semiconductor and becomes metallic while increasing the temperature. At the same time, it undergoes gradual LS to IS and then IS to HS transitions at around 100 K and 500 K, respectively.^{9,10}

Interestingly, external stimuli such as temperature, hydrostatic pressure, and cationic substitution allow the tuning of these spin states.^{11,12} In $\text{La}_{1-x}\text{M}_x\text{CoO}_3$ ($\text{M} = \text{Ca}, \text{Sr}, \text{Ba}$), the substitution of La^{3+} by M^{2+} ions that creates Co^{4+} ions modifies the spin state at the Co sites allowing to a mixture of spin states. Indeed similarly to Co^{3+} , Co^{4+} ($3d^5$) are also characterized by LS, IS, and HS states with orbital occupancy being $t_{2g}^5e_g^0$ ($S=1/2$), $t_{2g}^4e_g^1$ ($S=3/2$), and $t_{2g}^3e_g^2$ ($S=5/2$), respectively.¹⁰ For instance, Wu *et al.* showed that an increase in temperature and hydrostatic pressure leads to spin transition in Co^{3+} and Co^{4+} ions.⁴ The increasing of the temperature enhanced the depopulation of LS state of the Co^{3+} and the population of HS spin state. Moreover, at high enough pressure, it is found that the Co^{4+} can also undergo a spin-state transition (from IS to LS), in addition to that affecting the Co^{3+} (HS to LS).⁴ Similar results were proven in Refs. 13–17. It is worth mentioning that while some clustering (short-range order) exists for low doping ($x < 0.20$) an itinerant ferromagnetism at long-range order appears above $x \sim 0.2$ in these doped cobaltite likely due to Co^{3+} - Co^{4+} double exchange interactions. Since spin-orbital lattice interactions are important in such electron correlated systems, the magnetic and electronic transport properties can be varied

through lattice and/or symmetry modifications^{11,18,19} opening the path toward the design of properties on demand. For example, the IS state of both Co^{3+} and Co^{4+} ions is expected to be Jahn–Teller (JT) active, i.e., sensitive to CoO_6 octahedra distortions leading to a breaking of the six fold symmetry. Therefore being able to stabilize or destabilize JT effect by affecting such distortions would allow to tune the spin state and in turn the physical properties. Actually in $\text{La}_{1-x}\text{M}_x\text{CoO}_3$, JT can be stabilized in a wide range of hole doping x ²⁰ except for the composition $x = 0.3$ ^{11,20,21} where JT distortions are absent. For instance, using Raman spectroscopy at room temperature, Ishikawa *et al.* showed that the vibration modes assigned to JT distortions in LaCoO_3 are suppressed in $\text{La}_{0.7}\text{Sr}_{0.3}\text{CoO}_3$.²¹ This exception is a consequence of the onset of the created metallic state that destabilized JT effect by delocalizing the electrons.²⁰ Surprisingly, like for bulk $\text{La}_{0.7}\text{Sr}_{0.3}\text{CoO}_3$, JT distortion is also suppressed for bulk $\text{La}_{1-x}\text{Ca}_x\text{CoO}_3$ or $\text{La}_{1-x}\text{Ba}_x\text{CoO}_3$ ¹¹ while the distortions imposed by the ionic size of the dopant also impact the different structural, magnetic, and electronic transport properties in those latter systems.¹¹ Actually, the M-cation substitution acts like a chemical pressure. Note that it has been shown that a moderate hydrostatic pressure of the order of few kbars affects the JT-like magnetic transition through the change of spin states revealing the crucial role of the lattice distortion.²² Therefore, as in thin films the epitaxial misfit stress can reach until tens of kbar, it is of interest to investigate the consequences on the structure and thus the spin states when cobaltites are subjected to a biaxial stress. Combining chemical stress arising from substitution and mechanical stress by choosing appropriate substrate may appear as a powerful means for controlling spin states.²³

In this paper, we investigate how the strain effect and the temperature modify the occupancy of spin populations and their relation with physical properties in $\text{La}_{0.7}\text{Ba}_{0.3}\text{CoO}_3$ (LBCO) thin films. We show a clear anomalous temperature dependence correlating the Raman modes with magnetic transitions at about 210 K. Moreover, we demonstrate that the temperature evolution of the spin state revealed by Raman spectroscopy is directly linked to the structural deformation as revealed by X-ray diffraction stressing that the lattice distortion is indeed the driving force controlling the spin state and its resulting properties, i.e., magnetism and electronic transport.

II. EXPERIMENTAL

Here, we present such a study on a 100 nm-thick $\text{La}_{0.7}\text{Ba}_{0.3}\text{CoO}_3$ (LBCO) thin films coherently grown along [001]-direction on (001) LaAlO_3 (LAO) substrate using metal organic deposition (MOD) technique. The MOD technique has been revealed to be an efficient technique for epitaxial growth of cobaltite.^{24,25} $\text{La}_{0.7}\text{Ba}_{0.3}\text{CoO}_3$ has been chosen because it corresponds to the composition at which JT is suppressed in the bulk, as mentioned previously. The starting solution was prepared by diluting the preliminary mixed constituent metal-naphthenate solution (Nihon Kagaku Sangyo) with toluene to obtain the required concentration and viscosity. The molar ratios of La, Ba, and Co in the

coating solution were 0.7, 0.3, and 1.0, respectively. This solution was spin-coated onto LAO (001) substrate at 4000 rpm for 10 s. To eliminate the toluene, the metal-organic film was then dried in air at 100 °C for 10 min. Before the final annealing, a preheating step at 500 °C for 30 min is necessary to decompose the organic part.²⁴ This preheating step is also required to prevent the formation of cracks on the film surface during the final annealing at high temperature. The previous procedure (i.e., coating, drying, and preheating) was repeated 5 times giving rise to a corresponding number of superimposed layers to form the LBCO film. The final annealing was carried out in a conventional furnace at 800 °C for 60 min in air. The film thickness is estimated to be about 100 nm.^{24,25} The as-prepared film is free of any parasitic phases and although increasing the thickness is known to relax partially the epitaxial stress, the films still feel the substrate clamping allowing a well-oriented growth along pseudo-cubic [001]-direction.²⁶ Combining temperature dependent X-ray diffraction and Raman spectroscopy techniques, we have determined the structural changes and the vibration modes evolution in LBCO revealing insights into both lattice and spin states. The X-ray diffraction measurements were performed using a homemade two-axis X-ray diffractometer in Bragg–Brentano geometry with $\text{Cu K}_{\alpha 1}$ radiation issued from a 18 kW rotating anode (Rigaku) allowing an accuracy angle better than 0.002° in 2θ . The temperature was varied between 100 K and 700 K with a temperature precision better than 1 K, and selected diffraction patterns between 46° and 49° in 2θ were recorded. The Raman spectra between 180 cm^{-1} and 750 cm^{-1} were measured in the backscattering configuration using a Labram spectrometer single monochromator at $\lambda = 633 \text{ nm}$ with a charge coupled device detector allowing a resolution of 1 cm^{-1} . We checked that the laser power did not produce significant heating or damage of the sample. The temperature was varied with a Linkam THMS600 cell from 80 K to 600 K.

III. RESULTS AND DISCUSSION

In general, the change with temperature of phonon vibration modes (frequency/intensity/linewidth) in the Raman spectra is the result of several contributions, including lattice expansion and/or contraction, spin-phonon coupling, anharmonic scattering, and phonon renormalization due to electron-phonon coupling. Like LaAlO_3 substrate, $\text{La}_{0.7}\text{Ba}_{0.3}\text{CoO}_3$ crystallizes in the $R\text{-}3c$ space group.^{18,27} In this rhombohedrally distorted perovskite structure, only $A_{1g} + 4E_g$ Raman modes are found to be active.²⁸ Figure 1 shows the Raman spectra for (xx) and (xy) polarization configurations (x and y are the pseudocubic crystallographic directions) measured at room temperature. In addition to the E_g vibration mode of the LAO substrate at about 490 cm^{-1} , five extra-modes can be observed in the (xx) configuration. Although expected to be inactive in $R\text{-}3c$ symmetry, these extra-modes indicate the presence of additional distortions lowering the local crystal structure symmetry. Moreover, the randomness of the charges/spin states introduced by substitution of La^{3+} by Ba^{2+} and the strain effect relaxes the selection rules; thus extra-modes are expected. These modes

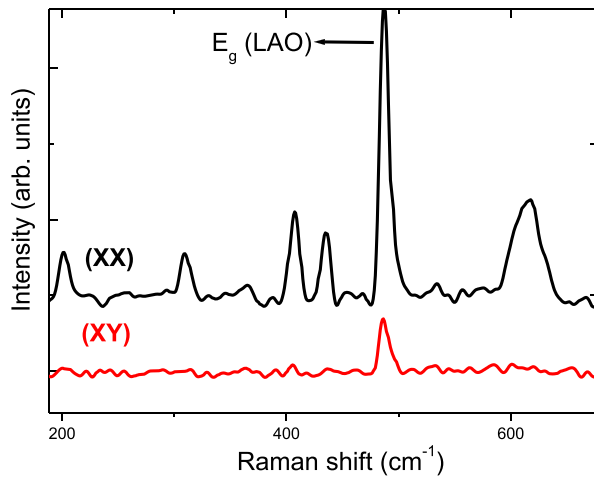


FIG. 1. Raman spectra at room temperature for (xx) and (xy) polarization configurations for the LBCO film grown on LAO substrate. The E_g mode of the LAO substrate is indicated.

become Raman active because the breaking of the symmetry due of the strain effects. In Figure 1, only the vibration mode of LAO is shown to be active for both configurations while the extra-modes disappear in (xy) polarization configuration. These modes have a similar behavior to Raman spectra observed in the parent compound LaCoO_3 .^{21,29} In case of the LaCoO_3 , the cooperative (even at short range order) JT effect is supposed to induce a change from $R-3c$ to monoclinic $C2/c$ space group²⁹ leading to the splitting of E_g modes into A_g and B_g modes. It appears that the stress imposed by the LAO substrate counteracts the chemical stress due to Ba-doping. In our opinion, the LBCO film could be of different symmetry than the $R-3c$ (symmetry of the bulk²⁷). Most likely the strain effect and the stress introduced by the substitution of La^{3+} by Ba^{2+} bring a stabilization of the JT distortions and create a relaxation of the selection rules. Therefore, let us now investigate whether the epitaxial stress may affect the vibrational properties as a function of temperature in the case of the LBCO. To this goal, we have measured Raman spectra at different temperatures varying between 90 K and 600 K. Figure 2 displays some Raman spectra at

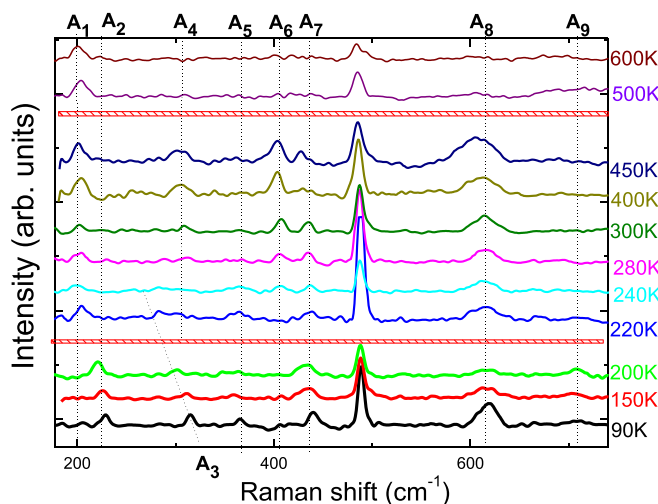


FIG. 2. Raman spectra versus temperature for LBCO film on LAO.

given temperatures. For the sake of clarity, in addition to the E_g LAO-mode, we labeled the extra-modes as A_i ($i = 1$ to 9). Three regions can be identified according to the vibration modes temperature dependence as shown in Figure 3, where the A_i Raman mode peak positions are plotted versus temperature. The region (I) ranging between ~ 90 K and ~ 210 K is characterized by 6 modes (A_2 , A_3 , A_5 , A_7 , A_8 , and A_9). In the region (II), i.e., for temperatures between ~ 210 K and ~ 500 K, the modes (A_2 , A_3 , A_5 , and A_9) vanish while new modes (A_1 , A_4 , and A_6) appear. Finally, in the region (III), i.e., above ~ 500 K, only mode A_1 persists. In bulk LBCO, a paramagnetic to ferromagnetic transition at a critical temperature $T_C \sim 200$ K was reported.²⁷ It is worth noting that biaxial pressure has an important influence in lattice structure, magnetism, and electron mobility.³⁰⁻³² Therefore, the electronic configuration of the d orbitals is disturbed by the stress and temperature which act on the energy levels of the d orbitals and thus affect the phase transitions.³² For instance by using magnetic measurements,²² Fita *et al.* showed that the hydrostatic pressure P shifts up the transition temperature in bulk $\text{La}_{0.7}\text{Ba}_{0.3}\text{CoO}_3$ as following: $T_c = 200.7 + 0.83P$. Assuming that the biaxial substrate stress can be approximated to a hydrostatic pressure, then the critical temperature we estimated from our data being $T_c \sim 210$ K may correspond to an equivalent pressure of ~ 10 kbar, which is close to the stress determined by X-ray diffraction as we will see later on.

Based on the phonon energies assignment reported in the literature,^{13,21,33,34} we discuss in the following the symmetry of the Raman modes observed in our LBCO film. The notation A_{1g} and E_g related to $R-3c$ space group to distinguish the phonon modes while the structure has a lower symmetry. It turns out that A_1 and A_2 modes correspond to the E_g vibrational modes of La/Ba atoms along the pseudocubic a - and b -axes, respectively. A_3 and A_4 are associated with A_{1g} rotation of the CoO_6 oxygen octahedra around c -axis. A_5 and A_6 are E_g bending modes. The A_7 mode in regions (I) and (II) has the same character as E_g (IS) but its energy is lower compared with LaCoO_3 .²¹ The atomic displacements correspond to the JT distortions in the IS state and are characterized by A_8 associated to E_g quadrupole mode in both

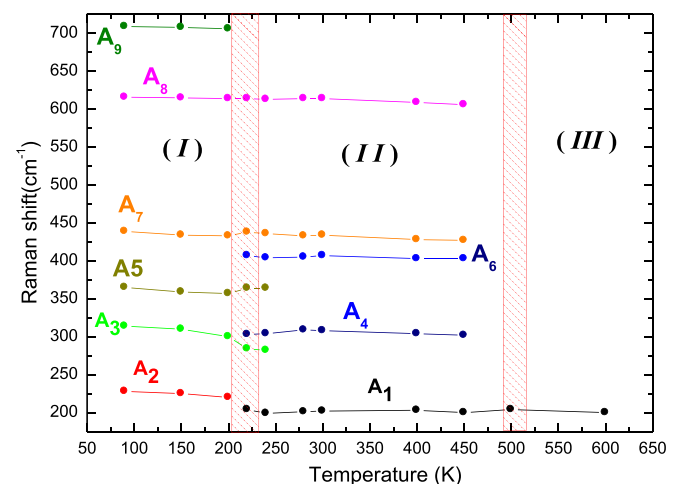


FIG. 3. Temperature dependence of phonon positions.

regions (I) and (II). The A_9 mode that appears only in region (I) is assigned to A_{2g} mode which is a silent mode becoming Raman active because of the relaxation of the selection rules aforementioned. We point out that the energy shifts of the vibrational modes observed in our films are larger than that in the bulk material.²¹ This may be related to the Ba-doping as well as the strain imposed by the underneath LAO substrate. Kozlenko *et al.*¹³ showed that the energy of the vibration modes increases with the application of a hydrostatic pressure. These position shifts in LBCO film may be due to the stress imposed by the LAO substrate. Nevertheless, it should be noted that La^{3+} substitution by Ba^{2+} may also induce chemical pressure due to the larger Ba^{2+} atomic radius. Indeed, both epitaxial and chemical stresses are believed to affect the spin states of this cobaltite and thus one can use such combined approach to design cobaltite properties on demand. On the other hand, the calculated phonon frequencies presented by Mukhopadhyay *et al.* in Ref. 35 show that the number of Raman active modes and their frequencies are strongly dependent on the spin states. Based on this study, we can associate the presence of the Raman modes (A_1 , A_9) to mixed spin phase (MS) in which LS, IS, and HS spin states coexist on different cobalt ions in the regions I and II. It is clear that the disappearance of the majority of modes in region III indicated the stability of states of the spins states of cobalt ions in one of the states. The most likely states are the HS because of the high temperature measurements in this region.

Let us now look at the evolution of vibration modes as the temperature is increased and show how the variations in

these modes are influenced by the spin transitions. The crystal field splitting Δ_{cf} decreases as the temperature increases, whereas the exchange interaction J_{ex} is insensitive to temperature. Therefore, based on the Raman mode temperature evolution, it can be proposed that the spin-state in LBCO (Co^{3+} and Co^{4+} ions) exhibits a gradual crossover with increasing temperature from the MS to HS spin state at 500 K. As a matter of fact, by increasing the temperature the value Δ_{cf} decreases and thus electrons populate the higher energy e_g orbitals. The anomalous temperature dependence in Raman spectra around 210 K correlating with the magnetic transitions. This concomitance of the vibrational transitions and the magnetic transitions indicates a substantial spin-lattice interaction in this LBCO thin film.

Let us now investigate the spin state transitions through their consequences on the structure by measuring the out-of-plane lattice parameter as a function of the temperature. Here, we would like to clarify if the transitions we observed by Raman spectroscopy at around 210 K and 500 K are associated to any structural distortion as expected for spin transition effects. Previous structural characterizations²⁶ showed that the single phased-LBCO films are epitaxially grown such as the in-plane a and b pseudo-cubic lattice parameters are constrained by the substrate. Because the LBCO thin film is clamped in-plane, all structural changes resulting from the thermal expansion and the phase transition are accommodated through changes in the out-of-plane lattice parameter only. Typical θ - 2θ diffraction patterns in the theta angle corresponding to LBCO (002) and LAO (002) Bragg reflections are displayed in Figure 4 between 100 K and 700 K. No peak

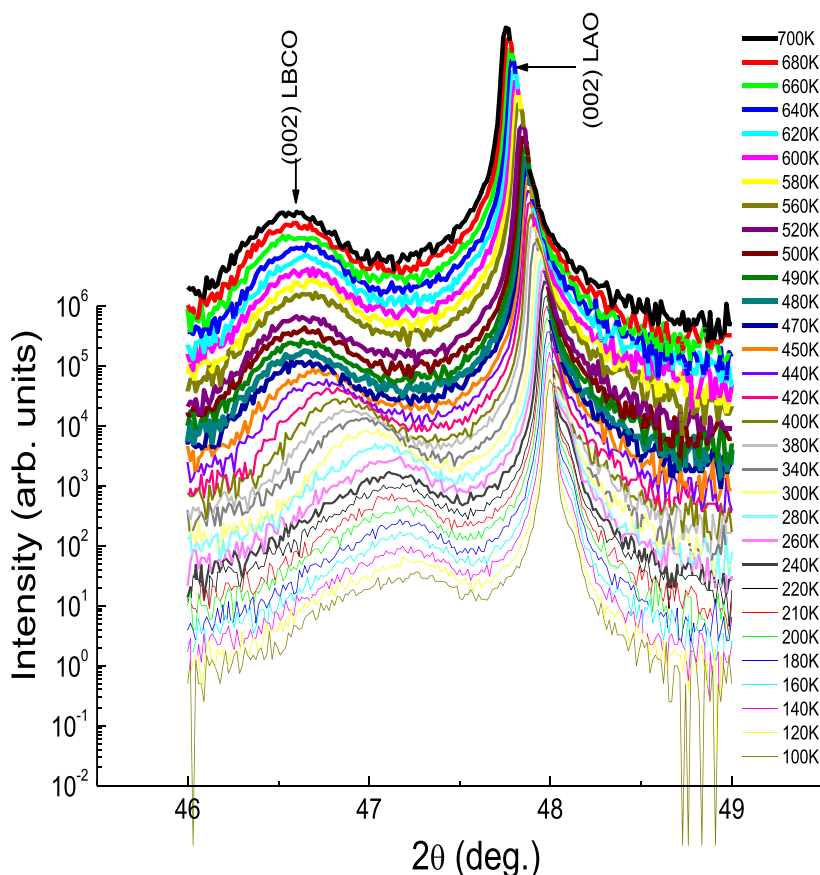


FIG. 4. θ - 2θ X-ray diffraction patterns around the pseudo-cubic (002) Bragg peaks versus temperature for LBCO film grown on LAO.

splitting is observed and thus we can extract from these data the pseudo-cubic out-of-plane parameter of our film. In order to extract an absolute value of the lattice parameter, a correction (zero, centring) was performed at room temperature by using five {001} Bragg peaks. The out-of-plane lattice parameter found at room temperature is 3.86 Å while the bulk pseudo-cubic value is 3.84 Å.²⁸ Given a Poisson coefficient of 0.33,³⁶ this enhancement of the out-of-plane lattice parameter corresponds to a compressive strain of 0.52%. Therefore, the stress felt by the film is estimated to 7.3 kbar by taking a Young's modulus of 140 GPa.³⁷ This value is in line with the one we found in the Raman analysis. Let us now look at the temperature dependence of the lattice parameter. Note that the Bragg peak associated to the substrate (not shown here) evolves linearly with the temperature range investigated as expected from its thermal expansion. In contrast, Figure 5 shows that the out-of-plane lattice parameter of LBCO extracted from the (002) Bragg peak displays two anomalies that are directly connected to 210 K and 500 K transition temperatures evidenced by Raman analysis. Obviously, these two lattice parameters changes attest to structural distortions which are concomitant with the spin states changes evidenced by Raman spectroscopy. Therefore, it is proposed that such distortions are the result of reduction of the Co-O-Co angle around T_c ^{38,39} at 210 K and spin transition at 500 K. LBCO film which is associated with preferential in-plane $d_{x^2-y^2}$ orbital occupation is induced. Then, strain effect enhances the hybridization between Co e_g and O $2p$ orbitals which in turn decreases the in-plane Co-O distance stabilizing the IS.⁴⁰⁻⁴² As a consequence, an elongation along the out-of-plane c -axis occurs. Approaching 210 K, the IS state contribution finally decreases in favor of the LS one allowing the semiconductor state to emerge instead of the metallic one as was observed in case of bulk LaCoO_3 using electrical resistivity and compressive strain measurements.^{12,43} Note that in Ref. 43, the mechanical measurements performed on LaCoO_3 have shown the two spin state transitions through thermal expansion coefficient which is fully in line with diffraction data observations.

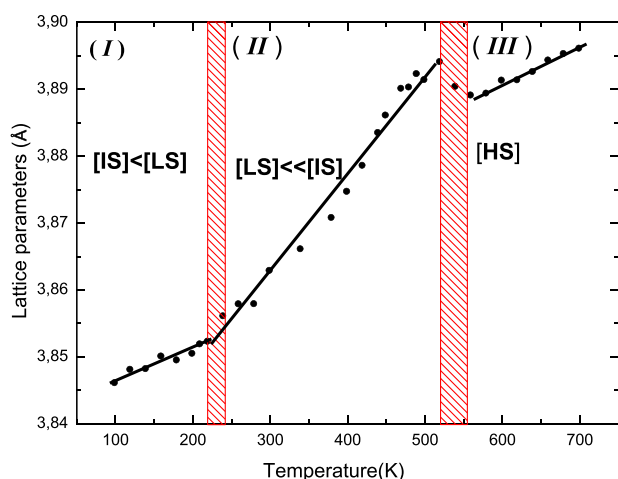


FIG. 5. Evolution of the out-of-plane lattice parameter of the LBCO film versus temperature.

IV. CONCLUSIONS

In summary, we have investigated that the temperature dependence of the Raman modes correlates with magnetic transition properties. It is clear that the concomitant of the vibrational transitions and the magnetic transition indicates a substantial spin-lattice interaction in this system. The compressive stress imposed by LAO substrate epitaxial and the chemical stresses affects the electronic configuration of the d orbitals. The magnetic transition and spin states transition at 210 K and 500 K, respectively, are detected in both techniques stressing the powerfulness of Raman spectroscopy to probe the spin states ion cobaltites. It appears finally that combining both epitaxial and chemical stresses can lead to efficient tuning of the spin states and thus the magnetic and electronic properties, a path that we believe should be considered much more considered in future researches.

- ¹J. Androulakis, P. Migiakis, and J. Giapintzakis, *Appl. Phys. Lett.* **84**, 1099 (2004).
- ²M. A. Torija, M. Sharma, J. Gazquez, M. Varela, C. He, J. Schmitt, J. A. Borchers, M. Laver, S. El-Khatib, and C. Leighton, *Adv. Mater.* **23**, 2711 (2011).
- ³M. Kubicek, Z. Cai, W. Ma, B. Yildiz, H. Hutter, and J. Fleig, *ACS Nano* **7**, 3276 (2013).
- ⁴J. Wu and C. Leighton, *Phys. Rev. B* **67**, 174408 (2003).
- ⁵V. Aswin, A. Dogra, A. Gupta, and J. J. Pulikkotil, *RSC Adv.* **6**, 1403 (2016).
- ⁶J. B. Goodenough and P. M. Raccach, *J. Appl. Phys.* **36**, 1031 (1965).
- ⁷C. Zobel, M. Kriener, D. Bruns, J. Baier, M. Grüninger, T. Lorenz, P. Reutler, and A. Revcolevschi, *Phys. Rev. B* **66**, 020402(R) (2002).
- ⁸S. Yamaguchi, Y. Okimoto, H. Taniguchi, and Y. Tokura, *Phys. Rev. B* **53**, R2926 (1996).
- ⁹M. A. Señaris-Rodríguez and J. B. Goodenough, *J. Solid State Chem.* **116**, 224 (1995).
- ¹⁰D. Fuchs, P. Schweiss, P. Adelman, T. Schwarz, and R. Schneider, *Phys. Rev. B* **72**, 014466 (2005).
- ¹¹D. Phelan, D. Louca, K. Kamazawa, M. F. Hundley, and K. Yamada, *Phys. Rev. B* **76**, 104111 (2007).
- ¹²J. W. Freeland, J. X. Ma, and J. Shi, *Appl. Phys. Lett.* **93**, 212501 (2008).
- ¹³D. P. Kozlenko, N. O. Golosova, Z. Jiráček, L. S. Dubrovinsky, B. N. Savenko, M. G. Tucker, Y. Le Godec, and V. P. Glazkov, *Phys. Rev. B* **75**, 064422 (2007).
- ¹⁴T. Das and T. Saha-Dasgupta, *Dalton Trans.* **44**, 10882–10887 (2015).
- ¹⁵F. Guillou, Q. Zhang, Z. Hu, C. Y. Kuo, Y. Y. Chin, H. J. Lin, C. T. Chen, A. Tanaka, L. H. Tjeng, and V. Hardy, *Phys. Rev. B* **87**, 115114 (2013).
- ¹⁶A. Podlesnyak, S. Streule, J. Mesot, M. Medarde, E. Pomjakushina, K. Conder, A. Tanaka, M. W. Haverkort, and D. I. Khomskii, *Phys. Rev. Lett.* **97**, 247208 (2006).
- ¹⁷M. W. Haverkort, Z. Hu, J. C. Cezar, T. Burnus, H. Hartmann, M. Reuther, C. Zobel, T. Lorenz, A. Tanaka, N. B. Brookes, H. H. Hsieh, H.-J. Lin, C. T. Chen, and L. H. Tjeng, *Phys. Rev. Lett.* **97**, 176405 (2006).
- ¹⁸P. Mandal, P. Choudhury, S. K. Biswas, and B. Ghosh, *Phys. Rev. B* **70**, 104407 (2004).
- ¹⁹A. Podlesnyak, M. Russina, A. Furrer, A. Alfonsov, E. Vavilova, V. Kataev, B. Buchner, Th. Strassle, E. Pomjakushina, K. Conder, and D. I. Khomskii, *Phys. Rev. Lett.* **101**, 247603 (2008).
- ²⁰N. Sundaram, Y. Jiang, I. E. Anderson, D. P. Belanger, C. H. Booth, F. Bridges, J. F. Mitchell, Th. Proffen, and H. Zheng, *Phys. Rev. Lett.* **102**, 026401 (2009).
- ²¹A. Ishikawa, J. Nohara, and S. Sugai, *Phys. Rev. Lett.* **93**, 136401 (2004).
- ²²I. Fita, R. Szymczak, R. Puzniak, A. Wisniewski, I. O. Troyanchuk, D. V. Karpinsky, V. Markovich, and H. Szymczak, *Phys. Rev. B* **83**, 064414 (2011).
- ²³D. W. Jeong, W. S. Choi, S. Okamoto, J.-Y. Kim, K. W. Kim, S. J. Moon, D.-Y. Cho, H. N. Lee, and T. W. Noh, *Sci. Rep.* **4**, 6124 (2014).
- ²⁴K. Daoudi, T. Tsuchiya, T. Nakajima, A. Fouzri, and M. Oueslati, *J. Alloys Compd.* **506**, 483 (2010).
- ²⁵K. Daoudi, T. Tsuchiya, I. Yamaguchi, T. Manabe, S. Mizuta, and T. Kumagai, *J. Appl. Phys.* **98**, 013507 (2005).

- ²⁶Z. Othmen, A. Schulman, K. Daoudi, M. Boudard, C. Acha, H. Roussel, M. Oueslati, and T. Tsuchiya, *Appl. Surf. Sci.* **306**, 60 (2014).
- ²⁷P. Tong, J. Yu, Q. Huang, K. Yamada, and D. Louca, *Phys. Rev. Lett.* **106**, 156407 (2011).
- ²⁸M. V. Abrashev, A. P. Litvinchuk, M. N. Iliev, R. L. Meng, V. N. Popov, V. G. Ivanov, R. A. Chakalov, and C. Thomsen, *Phys. Rev. B* **59**, 4146 (1999).
- ²⁹G. Maris, Y. Ren, V. Volotchaev, C. Zobel, T. Lorenz, and T. T. M. Palstra, *Phys. Rev. B* **67**, 224423 (2003).
- ³⁰D. Fuchs, M. Merz, P. Nagel, R. Schneider, S. Schuppler, and H. von Löhneysen, *Phys. Rev. Lett.* **111**, 257203 (2013).
- ³¹D. Fuchs, C. Pinta, T. Schwarz, P. Schweiss, P. Nagel, S. Schuppler, R. Schneider, M. Merz, G. Roth, and H. v. Löhneysen, *Phys. Rev. B* **75**, 144402 (2007).
- ³²R. Lengsdorf, M. Ait-Tahar, S. S. Saxena, M. Ellerby, D. I. Khomskii, H. Micklitz, T. Lorenz, and M. M. Abd-Elmeguid, *Phys. Rev. B* **69**, 140403(R) (2004).
- ³³E. Granado *et al.*, *Phys. Rev. B* **58**, 11435 (1998).
- ³⁴N. O. Golosova, D. P. Kozlenko, A. I. Kolesnikov, V. Yu. Kazimirov, M. B. Smirnov, Z. Jiráč, and B. N. Savenko, *Phys. Rev. B* **83**, 214305 (2011).
- ³⁵S. Mukhopadhyay, M. W. Finnis, and N. M. Harrison, *Phys. Rev. B* **87**, 125132 (2013).
- ³⁶D. Fuchs, E. Arac, C. Pinta, S. Schuppler, R. Schneider, and H. v. Löhneysen, *Phys. Rev. B* **77**, 014434 (2008).
- ³⁷S. Pathak, J. Kuebler, A. Payzant, and N. Orlovskaya, *J. Power Sources* **195**, 3612 (2010).
- ³⁸A. M. Durand, D. P. Belanger, C. H. Booth, F. Ye, S. Chi, J. A. Fernandez-Baca, and M. Bhat, *J. Phys.: Condens. Matter* **25**, 382203 (2013).
- ³⁹J. Buckeridge, F. H. Taylor, and C. R. A. Catlow, *Phys. Rev. B* **93**, 155123 (2016).
- ⁴⁰D. Louca and J. L. Sarrao, *Phys. Rev. Lett.* **91**, 155501 (2003).
- ⁴¹J. M. Rondinelli and N. A. Spaldin, *Phys. Rev. B* **79**, 054409 (2009).
- ⁴²M. A. Korotin, S. Yu. Ezhov, I. V. Solovyev, V. I. Anisimov, D. I. Khomskii, and G. A. Sawatzky, *Phys. Rev. B* **54**, 5309 (1996).
- ⁴³W. Araki, T. Abe, and Y. Arai, *J. Appl. Phys.* **116**, 043513 (2014).